

## Temporal and Spatial Distribution of DNA Topoisomerase II Alters During Proliferation, Differentiation, and Apoptosis in HL-60 Cells

By Koichi Sugimoto, Konagi Yamada, Motoki Egashira, Yoshio Yazaki, Hisamaru Hirai, Akihiko Kikuchi, and Kazuo Oshimi

We related cellular content of DNA topoisomerase (topo) II $\alpha$  and II $\beta$  with the cell cycle position in proliferating, differentiated, and apoptotic HL-60 cells using two-dimensional flow cytometry. In logarithmically growing HL-60 cells, topo II $\alpha$  increased especially in late S to G2/M phases, although the topo II $\beta$  level was almost constant throughout the cell cycle. Induction of differentiation by all-*trans* retinoic acid dramatically reduced the topo II $\alpha$  but not the topo II $\beta$  level. A new G2/M population containing virtually no topo II $\alpha$  appeared during differentiation and was supposed to be alive and noncycling. Two-dimensional flow cytometry of topo II $\alpha$  or II $\beta$  staining and terminal deoxynucleotidyl transferase-mediated dUTP-biotin nick end-labeling assay showed that one topo II $\beta$  epitope situated at the C-terminal end decreased specifically in apoptotic HL-60 cells treated with Ara-C, etoposide, and vincristine. The amounts of a topo II $\alpha$  epitope and another topo II $\beta$  epitope located at a more central portion were almost equal between apoptotic and

nonapoptotic cells. Western blot analysis confirmed that topo II $\beta$  protein was completely degraded into smaller fragments and lost its C-terminal end during apoptosis. On the contrary, a large portion of topo II $\alpha$  remained of its original size, although both topo II $\alpha$  and II $\beta$  left from the nuclear fraction in apoptotic cells. Confocal laser microscopy showed nuclear localization of topo II $\alpha$  and II $\beta$  in growing HL-60 cells. Although topo II $\alpha$  and II $\beta$  were distributed throughout the cell during mitosis, only topo II $\alpha$  was densely concentrated in the mitotic chromosomes. Both enzymes were dissociated from the genomic DNA even at an early phase of apoptosis and completely separated from the propidium iodide signal of DNA in the advanced stage. Chromatin condensation process in apoptosis is therefore completely topo II-independent and obviously differs from the mitotic one.

© 1998 by The American Society of Hematology.

**D**NA TOPOISOMERASE II (topo II) catalyzes the local changes in DNA topology by passing a double-stranded DNA helix through a transient double-strand break site and then rejoining the strand break.<sup>1,2</sup> Conditional yeast mutants in the *top2* gene showed that this enzymatic activity is required for segregation of daughter chromosomes during anaphase.<sup>3</sup> Biochemical studies using *Xenopus* egg extracts showed that topo II is essential for the condensation of interphase chromatin into metaphase chromosomes.<sup>4</sup> Treatment of mammalian cells with ICRF-193, which inhibits topo II activity without causing DNA damage, also leads to incomplete chromosomal condensation and segregation, resulting in polyploidy.<sup>5</sup> Topo II is the direct target of certain classes of antitumor agents. Etoposide and doxorubicin interact with topo II to inhibit the religation step of the enzyme, thereby stabilizing cleavable enzyme-DNA complexes that lead to DNA double-strand breaks and eventually to cell death.<sup>6</sup> Gene rearrangement in the MLL gene at chromosome 11q23 is frequently observed in chemotherapy-associated leukemias.<sup>7,8</sup> The break cluster region in this gene has been shown to coincide with the DNA cleavage sites specifically induced by topo II inhibitors *in vivo*.<sup>9,10</sup> Although only one topo II is known in yeasts and *Drosophila*, two isozymes of topo II have been identified in mammalian cells.<sup>1,11,12</sup> These two isozymes, topo II $\alpha$  (170-kD form) and topo II $\beta$  (180-kD form), with striking similarities in their amino acid sequences, are encoded by different genes. The topo II $\alpha$  staining showed fine punctuate fluorescence all over the nucleus except the nucleolar domain.<sup>13,14</sup> Although topo II $\beta$  was considered to exist preferentially in the nucleoli,<sup>14,15</sup> a recent report has shown that topo II $\beta$  is completely excluded from nucleoli.<sup>16</sup> The cellular concentration of topo II $\alpha$  but not topo II $\beta$  was reported to correlate with mitotic activity.<sup>17-19</sup> A decrease in cellular content of topo II $\alpha$  was previously reported during differentiation and E1A-induced apoptosis.<sup>20-22</sup>

Apoptosis is a distinct form of cell death that occurs in response to various stimuli, including DNA damage, withdrawal of growth factors, and inappropriate expression of genes

that stimulate cell cycle progression.<sup>23,24</sup> Apoptosis begins with condensation of nuclear chromatin at the nuclear periphery followed by blebbing of the nuclear and cytoplasmic membranes and culminates in the fragmentation of residual nuclear structures into discrete apoptotic bodies.<sup>23-25</sup> Although the regulation of apoptosis is complex, substantial evidence indicates that interleukin-1 $\beta$ -converting enzyme (ICE)-like proteases play a central role in this process.<sup>26,27</sup> Several nuclear proteins essential for DNA metabolism are specifically degraded by the action of the ICE-like proteases during apoptosis. These include poly (ADP-ribose) polymerase (PARP), nuclear lamins, DNA-dependent protein kinase catalytic subunit (DNA-PK cs), DNA topo I and II, NuMA, and RNA polymerase I upstream binding factor UBF.<sup>28-32</sup>

In this study, we showed a dramatic increase of topo II $\alpha$  but not topo II $\beta$  content in late S to G2/M phases in logarithmically growing HL-60 cells using two-dimensional flow cytometry. During differentiation, the majority of the HL-60 cells were

---

*From the Department of Hematology, Juntendo University School of Medicine, Tokyo, Japan; the Third Department of Internal Medicine, Faculty of Medicine, University of Tokyo, Tokyo, Japan; and the Laboratory of Medical Mycology, Research Institute of Disease Mechanism and Control, Nagoya University School of Medicine, Nagoya, Japan.*

*Submitted May 7, 1997; accepted October 16, 1997.*

*Supported by Grants-in-Aid for Cancer Research from the Ministry of Health and Welfare and from the Ministry of Education, Science and Culture in Japan.*

*Address reprint requests to Koichi Sugimoto, MD, Department of Hematology, Juntendo University School of Medicine, 2-1-1 Hongo, Bunkyo-ku, Tokyo 113, Japan.*

*The publication costs of this article were defrayed in part by page charge payment. This article must therefore be hereby marked "advertisement" in accordance with 18 U.S.C. section 1734 solely to indicate this fact.*

© 1998 by The American Society of Hematology.

0006-4971/98/9104-0021\$3.00/0

confined to G1/G0 position and simultaneously a new cell population emerged that contained tetraploid DNA and almost no topo II $\alpha$  protein. Two-dimensional flow cytometry combining topo II $\alpha$  or II $\beta$  staining with terminal deoxynucleotidyl transferase (TdT)-mediated dUTP-biotin nick end-labeling (TUNEL) assay suggested a decrease of a C-terminal but not a more central epitope of topo II $\beta$  in apoptotic HL-60 cells. Western blot analysis and immunostaining showed that both topo II $\alpha$  and II $\beta$  were rapidly dissociated from the chromatin in apoptotic HL-60 cells, although only topo II $\beta$  was extensively degraded during apoptosis.

## MATERIALS AND METHODS

**Monoclonal antibodies.** Preparations of topo II $\alpha$ -specific antibody 8D2 and topo II $\beta$ -specific antibodies 5A7 and 3G3 were described previously.<sup>22,33</sup> The epitope of 8D2 exists between amino acids 1260 and 1460 of topo II $\alpha$ . The epitopes of 5A7 and 3G3 are located in amino acids 1583 to 1601 and between amino acids 1260 and 1460 of topo II $\beta$ , respectively.

**Cell culture and drug treatment.** The HL-60 human myeloid leukemia cell line was maintained in RPMI 1640 (GIBCO BRL, Grand Island, NY) supplemented with 10% fetal calf serum, 100 U/mL penicillin, 100  $\mu$ g/mL streptomycin, and 2 mmol/L L-glutamine. The cells were split to keep the cell density at  $2 \times 10^5$  to  $1 \times 10^6$  cells/mL.

To induce cell differentiation, HL-60 cells were treated with 1  $\mu$ mol/L of all-*trans* retinoic acid (ATRA; Sigma, St Louis, MO) for 6 days. Cell density was kept at  $2 \times 10^5$  to  $1 \times 10^6$  cells/mL during the treatment. Logarithmically growing HL-60 cells were treated for the indicated times with cytosine b-D-arabino-furanose (Ara-C; 4  $\mu$ mol/L), etoposide (100  $\mu$ mol/L), or vincristine (0.2  $\mu$ mol/L) (all reagents were purchased from Sigma).

**Cell fixation.** In brief,  $1 \times 10^6$  cells were harvested by centrifugation for 8 minutes at room temperature at 400g, washed once with phosphate-buffered saline (PBS), and then fixed in 1% formaldehyde in PBS (pH 7.4) for 15 minutes on ice. After washing in PBS, cells were resuspended in 70% cold ( $-20^\circ\text{C}$ ) ethanol and immediately transferred to the freezer. The cells were stored at  $-20^\circ\text{C}$  for 1 day before being subject to the indirect immunofluorescence or TUNEL assay.

**Indirect immunofluorescence.** Cells were washed twice in PBS, incubated in 100  $\mu$ L of PBS containing 0.1% Triton X-100 for 5 minutes at room temperature, and blocked in 100  $\mu$ L of PBS containing 3% (wt/vol) nonfat dry milk for 30 minutes at room temperature. To detect topo II $\alpha$  and II $\beta$ , cells were incubated with a 1:30 dilution of 8D2 and 5A7, respectively, in PBS with 3% nonfat milk for 1.5 hours at room temperature. In some cases, 3G3 was used to detect topo II $\beta$  instead of 5A7. Cells were washed twice in PBS containing 0.1% Triton X-100 and then incubated in a 1:30 dilution of a fluorescein isothiocyanate (FITC)-conjugated goat-antimouse IgG (Ortho, Raritan, NJ) in PBS/3% milk solution for 1 hour at room temperature in the dark.

**TUNEL assay.** After rehydration in PBS, cells were resuspended in 50  $\mu$ L of a cacodylate buffer containing 0.2 mol/L potassium cacodylate, 25 mmol/L Tris-HCl (pH 6.6), 2.5 mmol/L CoCl<sub>2</sub>, 0.25 mg/mL bovine serum albumin, 5 U TdT, and 0.5 nmol of biotin-dUTP (all reagents were purchased from Boehringer Mannheim, Indianapolis, IN). The cells were incubated in this solution at  $37^\circ\text{C}$  for 30 minutes; rinsed in PBS; resuspended in 100  $\mu$ L of a solution containing 4 $\times$  concentrated saline-sodium citrate buffer, 2.5  $\mu$ g/mL fluoresceinated avidin (Boehringer Mannheim), 0.1% Triton X-100, and 5% (wt/vol) nonfat dry milk; and incubated in this solution for 30 minutes at room temperature in the dark. This procedure essentially followed the previous report by Gorczyca et al.<sup>34</sup>

**Flow cytometry.** After incubation in staining buffer, the cells were rinsed in PBS containing 0.1% Triton X-100 and resuspended in 1 mL

of PBS containing 5  $\mu$ g/mL of propidium iodide (PI) and 200  $\mu$ g/mL of RNase A (both from Sigma). Flow cytometry was performed on a CYTRON ABSOLUTE flow cytometer (Ortho). The orange (PI) and green (fluorescein isothiocyanate [FITC]) fluorescence emissions from each cell were separated and measured using the standard optics of the CYTRON ABSOLUTE. The data from  $5 \times 10^4$  cells were collected, stored, and analyzed. The signal of green fluorescence was measured using linear amplification for topo II $\alpha$  and II $\beta$  staining and using logarithmic amplification for the TUNEL assay.

**Two-dimensional flow cytometry of immunostaining and TUNEL assay.** After performing the TUNEL assay protocol described above, cells were rinsed twice in PBS containing 0.1% Triton X-100 and then resuspended in PBS/3% milk solution containing the primary antibody, 8D2 or 5A7. Thereafter, cells were stained with the same procedure for indirect immunostaining except that 1:50 dilution of phycoerythrin (PE)-conjugated goat-antimouse IgG (BioSource, Camarillo, CA) was used as a secondary antibody and that PI staining at the final step was omitted. In this case, topo II $\alpha$  and II $\beta$  signals of orange fluorescence were measured using linear amplification and the green fluorescence of TUNEL assay using logarithmic amplification.

**Western blot analysis.** Harvested cells were washed once with PBS and suspended in ice-cold buffer 1 (10 mmol/L HEPES, pH 7.9, 10 mmol/L KCl, 1 mmol/L EDTA, 1 mmol/L dithiothreitol [DTT], 0.05% Triton X-100, and 1 mmol/L phenylmethylsulfonyl fluoride [PMSF]) at the concentration of  $2 \times 10^7$  cells/mL. The suspension was kept on ice for 20 minutes, vortexed vigorously for 10 seconds to be lysed, and then spun down at 1,000g for 4 minutes at  $4^\circ\text{C}$ . The supernatant was recovered as a cytoplasmic fraction. The nuclear pellet was resuspended in the same volume of ice-cold nuclear extraction buffer 2 (20 mmol/L HEPES, pH 7.9, 400 mmol/L NaCl, 1 mmol/L EDTA, 1 mmol/L DTT, and 1 mmol/L PMSF), rocked on ice for 30 minutes, and centrifuged at 13,000g for 10 minutes at  $4^\circ\text{C}$ . The supernatant was recovered as a nuclear fraction. In every experiment in this study, the nuclear remnant was confirmed to contain essentially no topo II proteins by immunoblotting. Cytoplasmic and nuclear fractions derived from  $5 \times 10^5$  cells were separated on a 7% polyacrylamide gel. Immunoblotting was performed as described previously,<sup>35</sup> using a 1:200 dilution of 8D2, 5A7, and 3G3. As a second antibody, alkaline phosphatase-conjugated antimouse Ig (ProMega, Madison, WI) was used at the dilution of 1:5,000.

**Confocal laser microscopy.** The cells immunostained for flow cytometric analysis were rinsed in PBS containing 0.1% Triton X-100. An aliquot of the cells was resuspended in 200  $\mu$ L of PBS containing 200 ng/mL of PI and 200  $\mu$ g/mL of RNase A (both from Sigma), resuspended in 100  $\mu$ L of PBS, and then attached to a poly-L-lysine coated slide glass. The coverslip was mounted with 10  $\mu$ L of antifading mix (50% glycerol, 2.5% 1,4-diazabicyclo[2.2.2]octane [DABCO] in PBS) and sealed with nail polish. The slides were viewed and photographed through a Bio-Rad MRC-1024 confocal laser scanning microscope (Bio-Rad, Hercules, CA).

## RESULTS

The cellular contents of topoisomerase II $\alpha$  and II $\beta$  were studied using monoclonal antibodies 8D2 and 5A7. Specificities of 8D2 to topo II $\alpha$  and 5A7 to topo II $\beta$  were shown previously.<sup>22,23</sup> Two-dimensional flow cytometric analysis of cells indirectly fluorescein-labeled for topo II $\alpha$  or II $\beta$  and then counterstained with PI made it possible to quantify the amounts of topo II $\alpha$  or II $\beta$  and relate them to cellular DNA content, ie, to the cell cycle position. The DNA content histogram of logarithmically growing HL-60 cells contains two peaks: a large and sharp peak at G1 and the other small one at G2/M (Fig 1A). S phase cells distribute between these peaks forming a bridge shape. The cellular concentration of topo II $\alpha$  increases during the cell cycle progression and a steep increase is prominent

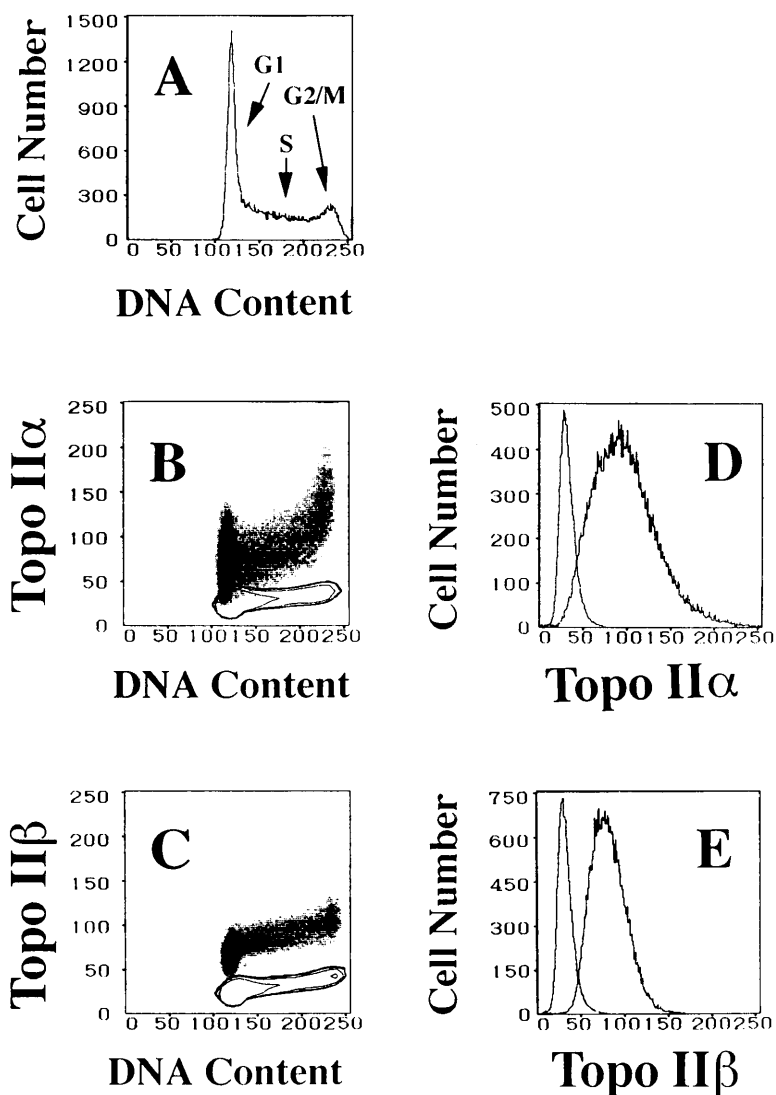


Fig 1. Alterations in topo II $\alpha$  and II $\beta$  levels in logarithmically growing HL-60 cells as a function of DNA content, ie, the cell cycle position. (A) DNA histogram showing the cell cycle distribution of logarithmically growing HL-60 cells. (B and C) Two-dimensional flow cytometric analyses of DNA content and topo II $\alpha$  and II $\beta$  signals, respectively. Isotype-matched negative controls are depicted as contour maps. (D and E) Histograms of topo II $\alpha$  and II $\beta$  contents, respectively. Isotype-matched control fluorescence curves are the most proximal to the Y-axis.

from late S to G2/M phases (Fig 1B). In G1 phase, topo II $\alpha$  content varies from almost zero to somewhat larger than that of early S phase. On the contrary, topo II $\beta$  level slightly increases in G1 phase and thereafter is not significantly altered through the cell cycle (Fig 1C). Although the topo II $\beta$  signal appears to increase even during the S phase, subtraction of the nonspecific binding fluorescence of an isotype-matched control antibody indicates that the topo II $\beta$  content is almost constant. When we compare the single parameter histograms of the two topo II enzymes, the range of distribution for topo II $\alpha$  signal was much wider than that of topo II $\beta$ , although these histograms peak at almost the same signal intensity (Fig 1D and E). These results were representative of five similar experiments.

Two-dimensional flow cytometric analysis on differentiating HL-60 cells showed alterations in the cell cycle distribution and changes in topo II $\alpha$  and II $\beta$  levels at each cell cycle position. We induced differentiation of HL-60 cells with the addition of 1  $\mu$ mol/L of ATRA to the culture medium for 6 days. More than 90% of the cells were confirmed to express CD11b on the cell surface by day 4 (data not shown). During differentiation, the

cell population belonging to S and G2/M phases gradually decreased, and only a small portion of the cells were found in S phase at day 6 (Fig 2A through D). By day 2, the amount of topo II $\alpha$  as a function of cell cycle position showed similar pattern to that of the nontreated cells, although the topo II $\alpha$  signal decreased slightly (Fig 2E and F). At day 4, a large portion of the cells were confined to G1 and a considerable part of these G1 cells no longer expressed topo II $\alpha$  enzyme (Fig 2C and G). A new cell population that belongs to G2/M phase and simultaneously contains almost no topo II $\alpha$  appeared at this stage, and this cell group became more prominent at day 6 (Fig 2G and H). Because a portion of the G0/G1 cells had a relatively high level of topo II $\alpha$  signal, as shown in Fig 2H, if the G2/M population were constituted of the clumped G0/G1 cells, some cells of this population should also contain a high level of topo II $\alpha$  signal. Actually, even when we increased the detection gain or the numbers of cells analyzed, the G2/M population in Fig 2H showed no upward tail, which corresponds to a cell group containing a rather high level of topo II $\alpha$  signal. Furthermore, we clearly detected this G2/M cell population by two-

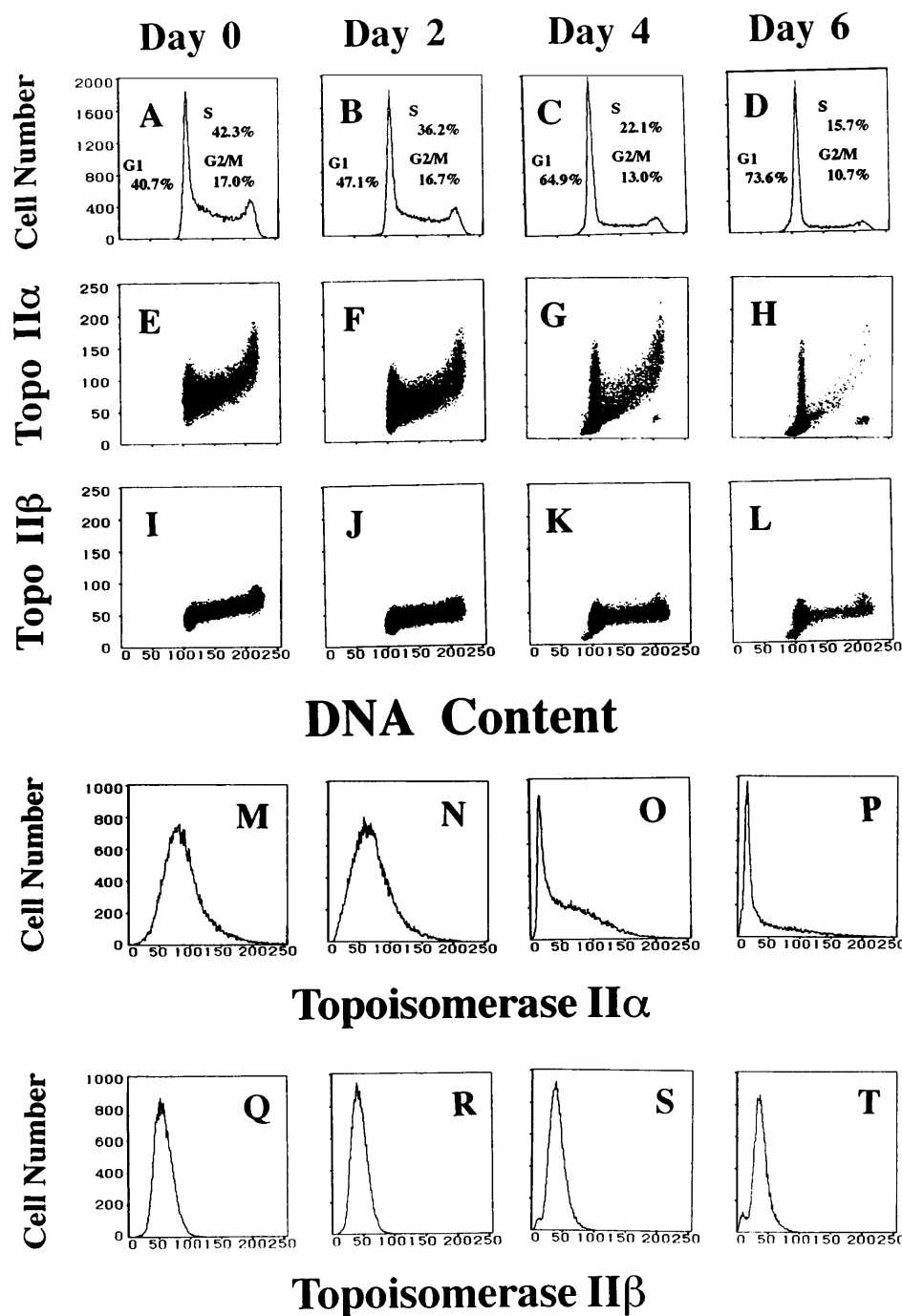


Fig 2. Topo II $\alpha$  level decreases dramatically and a new G2/M cell population expressing almost no topo II $\alpha$  emerges during the ATRA-induced differentiation. Logarithmically growing HL-60 cells are treated with 1  $\mu$ mol/L of ATRA, before the treatment (A, E, I, M, and Q), for 2 days (B, F, J, N, and R), for 4 days (C, G, K, O, and S), and for 6 days (D, H, L, P, and T). DNA histograms with insets showing the percentage of cells in each phase of the cell cycle (A through D). Two-dimensional flow cytometric analyses of DNA contents and topo II $\alpha$  and II $\beta$  signals (E through H and I through L, respectively). Histograms of topo II $\alpha$  and II $\beta$  contents (M through P and Q through T, respectively).

dimensional flow cytometry still after the gating to eliminate the clumped G0/G1 cells. In contrast with topo II $\alpha$ , the signal of topo II $\beta$  decreased a little at day 2 and essentially kept this level until day 6 (Fig 2I through L). At days 4 and 6, there appeared a sub-G1 population that contained almost no topo II $\beta$  (Fig 2K, L, S, and T). The results of TUNEL assay suggested that these cells were apoptotic (data not shown), which agrees with the results described below showing that 5A7 epitope of topo II $\beta$  specifically decreases during apoptosis. The single-parameter histograms confirmed that topo II $\alpha$  level decreased steeply and the peak shifted to the position of almost no topo II $\alpha$  signal at day 4

(Fig 2M through P). Topo II $\beta$  level was not so much altered during differentiation (Fig 2Q through T). Similar results were observed in three independent studies.

We next examined topo II $\alpha$  and II $\beta$  levels and related them with the cell cycle position in apoptotic HL-60 cells treated with antitumor drugs. The extent of DNA strand breaks, one of the hallmarks of apoptosis, was also correlated to the cell cycle position using the TUNEL assay combined with PI staining. We used three antitumor drugs with different mechanisms of action: pyrimidine analogue antimetabolite Ara-C, topo II inhibitor etoposide, and vinca alkaloid antimitotic agent vincristine.<sup>36</sup>

Based on the results of previous reports,<sup>31,37</sup> we experimentally determined the doses of Ara-C (4  $\mu\text{mol/L}$ ) and etoposide (100  $\mu\text{mol/L}$ ) that induce apoptosis in 50% to 80% of rapidly growing HL-60 cells in 6 to 8 hours (data not shown). Measured as an apoptotic cell percentage, 0.05  $\mu\text{mol/L}$  of vincristine had essentially the same effect as that of 4  $\mu\text{mol/L}$  (data not shown). We therefore treated HL-60 cells with 0.2  $\mu\text{mol/L}$  of vincristine. At this concentration, it took about 18 hours to induce apoptosis in more than 50% of the treated cells.

With the Ara-C treatment, the G2/M peak disappeared and a small peak at sub-G1 position emerged (Fig 3B). As a function of the cell cycle position, the topo II $\alpha$  level decreased a little in these cells (Fig 3F). On the contrary, Ara-C-treated cells were divided into two populations with nearly normal and very small topo II $\beta$  contents (Fig 3J). TUNEL-positive cells were distributed in sub-G1 to S phases, suggesting a partial loss of DNA stainability in apoptotic cells (Fig 3N). Most of the nonapoptotic cells were restricted in G1 phase. Comparison between Fig 3J and N suggests a possibility that the topo II $\beta$  signal should decrease specifically in apoptotic cells.

Etoposide-treated cells also lost the G2/M population and the G1 peak had a broader shoulder at sub-G1 side (Fig 3C). The topo II $\alpha$  level was somewhat decreased at any position in the

cell cycle (Fig 3G). Only part of the G1 cells contained a normal amount of topo II $\beta$  and all of the remaining cells had a decreased topo II $\beta$  signal (Fig 3K). TUNEL assay showed that only a portion of G1 cells were free from apoptosis (Fig 3O). Therefore, a decrease of the topo II $\beta$  signal also seemed to correlate with apoptosis in etoposide-treated HL-60 cells.

Treatment with vincristine confined HL-60 cells to late S and G2/M phases (Fig 3D). As a result, most of the cells expressed a higher level of topo II $\alpha$  than normal control (Fig 3H). As for topo II $\beta$ , these cells were divided into two populations with intact and decreased enzyme levels (Fig 3L). Both apoptotic and nonapoptotic cells were in late S to G2/M phases (Fig 3P).

To address the possible relationship between topo II $\beta$  level and apoptosis more directly, cells were labeled by the TUNEL assay, stained for topo II $\alpha$  or topo II $\beta$ , and then analyzed by two-dimensional flow cytometry. In Ara-C-treated HL-60 cells, a large portion of the apoptotic cells contained approximately the same amount of topo II $\alpha$  as the nonapoptotic ones (Fig 4B). On the contrary, the apoptotic cells apparently contained less topo II $\beta$ , with apoptotic and nonapoptotic populations essentially nonoverlapping as for the topo II $\beta$  level (Fig 4F). When we used etoposide, the apoptotic and nonapoptotic HL-60 cells expressed almost equal amounts of topo II $\alpha$  (Fig 4C). However,

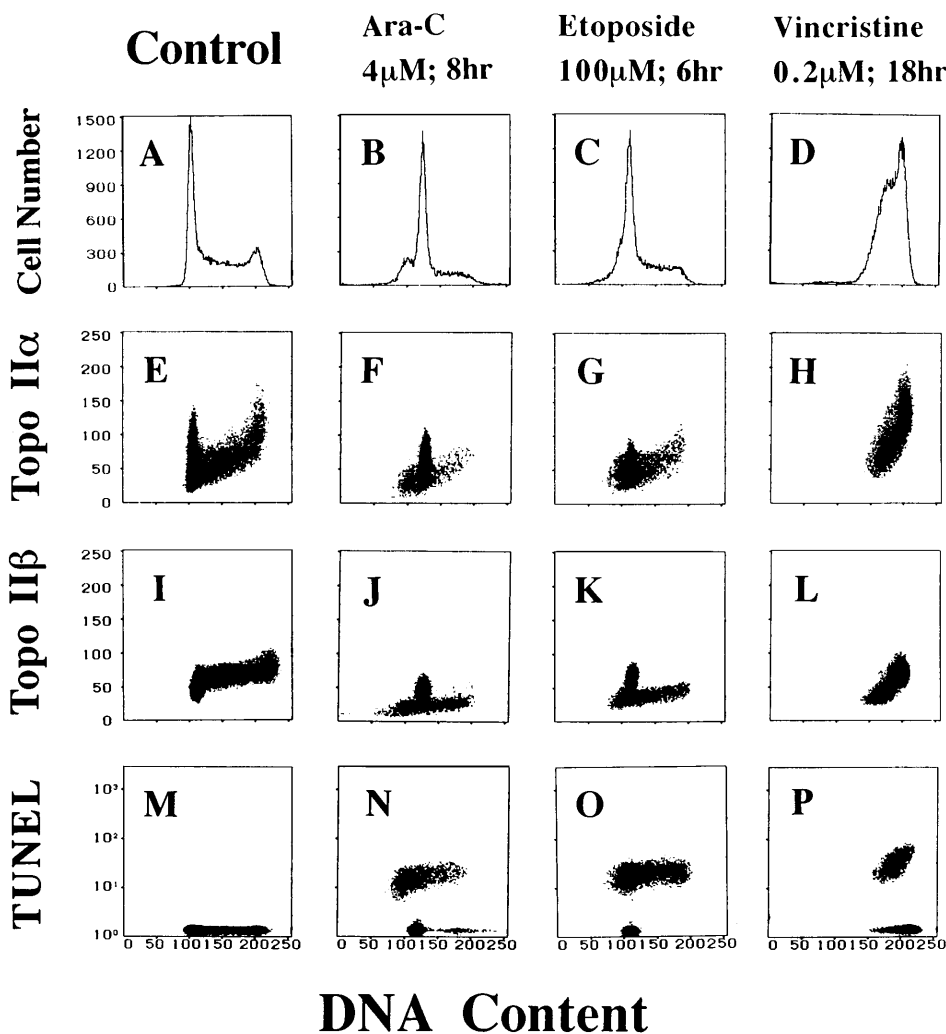


Fig 3. Antitumor drugs alter the cell cycle distribution and topo II $\alpha$  and II $\beta$  contents of HL-60 cells. DNA histograms (A through D), two-dimensional flow cytometric analyses of DNA-topo II $\alpha$  contents (E through H), DNA-topo II $\beta$  contents (I through L), and DNA content-TUNEL assay (M through P) of control and Ara-C-, etoposide-, and vincristine-treated HL-60 cells.

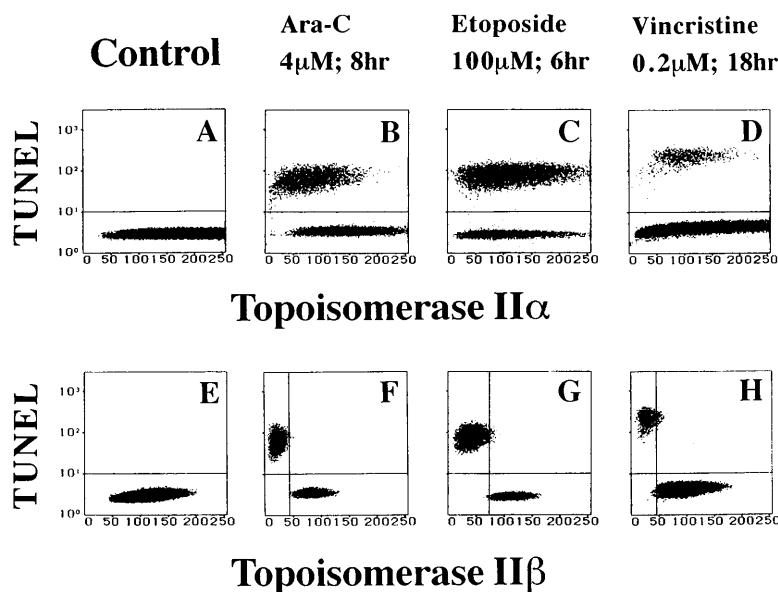


Fig 4. Topo II $\beta$  but not topo II $\alpha$  signal decreases specifically in apoptotic HL-60 cells treated with antitumor drugs. Two-dimensional flow cytometric analyses of topo II $\alpha$  and II $\beta$  contents and TUNEL assay (A through D and E through H, respectively).

the topo II $\beta$  level clearly separated these two populations (Fig 4G). Also, in vincristine-treated cells, although the apoptotic and nonapoptotic cells contained a similar level of topo II $\alpha$ , they differed sharply in their content of topo II $\beta$  (Fig 4D and H). Every result shown in Fig 3 and 4 was reproducibly obtained in at least three separate experiments. Because the three antitumor drugs used in this study have apparently different mechanisms of action, these observations indicate that a decrease in the topo II $\beta$  level is not a drug-specific event but a more general phenomenon accompanying the drug-induced apoptosis.

Because we used the monoclonal antibody 5A7 specific to the C-terminal portion of topo II $\beta$  (amino acids 1583 to 1601) in the experiments described above, we could not distinguish the two possibilities that the full molecule or only the N-terminal portion of topo II $\beta$  was lost during apoptosis. To investigate this question, we determined the topo II $\beta$  level of the Ara-C-treated HL-60 cells using a monoclonal antibody 3G3, which recognizes a more central epitope of topo II $\beta$  (between amino acids 1260 and 1460) than that of 5A7. Flow cytometry using 5A7 as a primary antibody clearly separated Ara-C-treated HL-60 cells into two populations with almost normal and decreased levels of topo II $\beta$  signal as shown above (Fig 5B). On the contrary, 3G3 did not discriminate between the apoptotic and nonapoptotic cells, both of which showed an almost normal level of topo II $\beta$  signal (Fig 5D). Similar results were obtained in three independent experiments. Etoposide-treated HL-60 cells also divided into apoptotic and nonapoptotic populations by 5A7 but not by 3G3 (data not shown). These results indicate that the 5A7 epitope at the C-terminal portion of topo II $\beta$  should be degraded or modified during apoptosis, although a more central 3G3 epitope of topo II $\beta$  was preserved.

We then investigated possible cleavages of topo II $\alpha$  and II $\beta$  during apoptosis by Western blot analysis using 8D2 and 5A7/3G3, respectively. The flow cytometric TUNEL analysis showed that approximately 50% of HL-60 cells underwent apoptosis after 5 hours of incubation with 4  $\mu$ mol/L of Ara-C (data not shown). In 10 hours, more than 95% of the treated cells were positive for the TUNEL assay (data not shown). We

separated rapidly growing and Ara-C-treated HL-60 cells into cytoplasmic and nuclear fractions with 0.05% Triton X-100. Each fraction was then subjected to immunoblotting. In logarithmically growing HL-60 cells, both topo II $\alpha$  and II $\beta$  were detected at their expected size (170 kD and 180 kD, respectively) exclusively in the nuclear fraction (0 hours; Fig 6A, B, and C). Although distribution of topo II $\alpha$  was completely changed from the nuclear to cytoplasmic fractions during the course of apoptosis, a large portion of topo II $\alpha$  remained of its

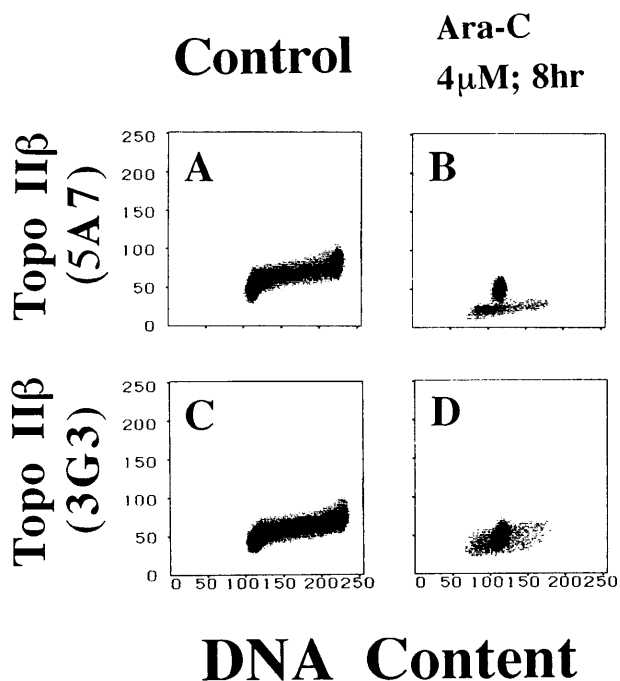
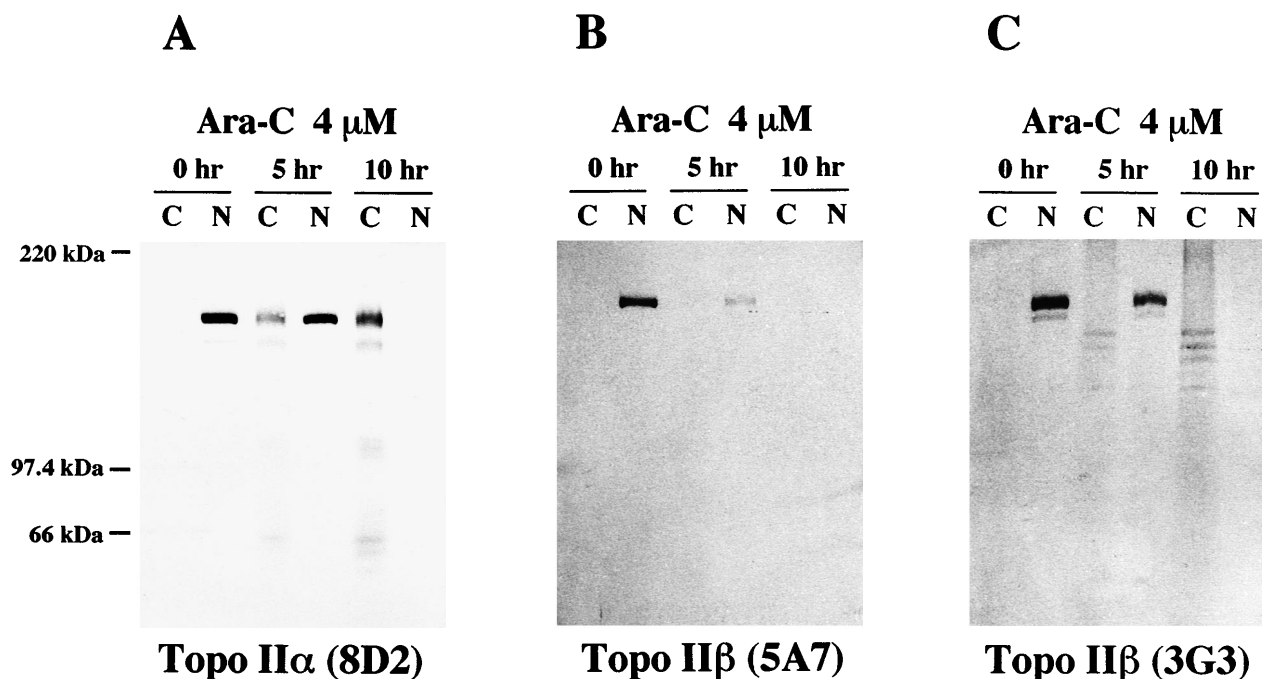


Fig 5. 5A7 but not 3G3 separates apoptotic HL-60 cells from nonapoptotic ones. Two-dimensional flow cytometric analyses of DNA-topo II $\beta$  contents are performed on logarithmically growing (A and C) and Ara-C-treated HL-60 cells (B and D) using topo II $\beta$ -specific monoclonal antibodies, 5A7 (A and B) and 3G3 (C and D).



**Fig 6.** Topo IIβ but not topo IIα is extensively degraded during the Ara-C-induced apoptosis. Western blot analyses of logarithmically growing HL-60 cells (0 hours) and those treated with 4 μmol/L of Ara-C for 5 and 10 hours (5 and 10 hr, respectively) with topo IIα-specific 8D2 (A) and topo IIβ-specific 5A7 and 3G3 monoclonal antibodies (B and C, respectively).

original size even in apoptotic cells (Fig 6A). Only a small amount of degraded topo IIα fragments were detected in the cytoplasmic fraction of the apoptotic cells. When we used 5A7 to detect topo IIβ, the 180-kD band in the nuclear fraction became faint in 5 hours and no bands were detected in either the cytoplasmic or nuclear fraction after 10 hours of incubation (Fig 6B). Another topo IIβ-specific antibody 3G3 showed the appearance of several smaller fragments of 125 to 160 kD in the cytoplasmic fraction besides a proportional reduction in the amount of the 180-kD band in the nuclear fraction after 5 hours of Ara-C treatment (0 and 5 hours; Fig 6C). The smaller fragments in the cytoplasmic fraction became more prominent and the intact 180-kD band disappeared in 10 hours (10 hours; Fig 6C), indicating that topo IIβ was completely degraded into these smaller fragments. Essentially the same results were obtained in three independent experiments and also in etoposide-treated cells with a slightly shorter time course (about 7 to 8 hours for complete apoptosis; data not shown). These results confirmed that the C-terminal 5A7 epitope is lost and a more central 3G3 epitope is preserved in the apoptotically degraded topo IIβ fragments. The Western blot analysis thus shows that a large portion of topo IIα remains of its original size even in apoptotic HL-60 cells, although intact topo IIβ is lost at an early phase of apoptosis.

Topo IIα and IIβ (fragments) moved completely from the nuclear to cytoplasmic fractions in apoptotic cells. Because the fractionation procedure was biochemical, the change in the distribution of topo II enzymes may have merely reflected a collapse of nuclear integrity. To investigate a probable change in the cellular localization of topo IIα and IIβ during apoptosis more directly, we immunostained intact and Ara-C-treated apoptotic HL-60 cells using 8D2 and 3G3 and then examined

them with confocal laser microscopy (Fig 7). Topo IIα-specific 8D2 and topo IIβ-specific 3G3 signals are visualized as green color and PI counterstained DNA red. In logarithmically growing cells, topo IIα and IIβ were localized in the nucleus showing a fine granular pattern except for the nucleoli (Fig 7A and C, respectively). Both topo II enzymes were distributed throughout the cell during mitosis (Fig 7A and D). Only topo IIα signal was concentrated in the mitotic chromosomes with merged intense yellow color. This observation was confirmed by the comparison of topo IIα signals in the chromosomes and in the mitotic cytoplasm (data not shown). When we stained HL-60 cells treated with Ara-C for 5 hours, some nuclei showed chromatin condensation at the nuclear periphery and others showed a typical apoptotic pattern with discrete apoptotic bodies. Topo IIα signal was dissociated from the chromatin at an early phase of apoptosis and completely separated from the bright red signal of DNA in an advanced stage (Fig 7B, upper and lower cells, respectively). Topo IIβ was also segregated from the chromatin even at an early stage of apoptosis (Fig 7E). These results were representative of three independent experiments conducted under similar conditions.

**DISCUSSION**

In this study, we showed temporal and spatial changes in topo IIα and IIβ distributions in proliferating, differentiated, and apoptotic HL-60 cells using two-dimensional flow cytometry, Western blot analysis, and confocal laser microscopy. At first, we related topo IIα and IIβ levels with the cell cycle position in logarithmically growing HL-60 cells. Although a previous study determined the contents of topo IIα and IIβ in synchronized cells at 2-hour intervals for a total of 28 hours, the cells were not so well restricted to narrow positions in the cell cycle,

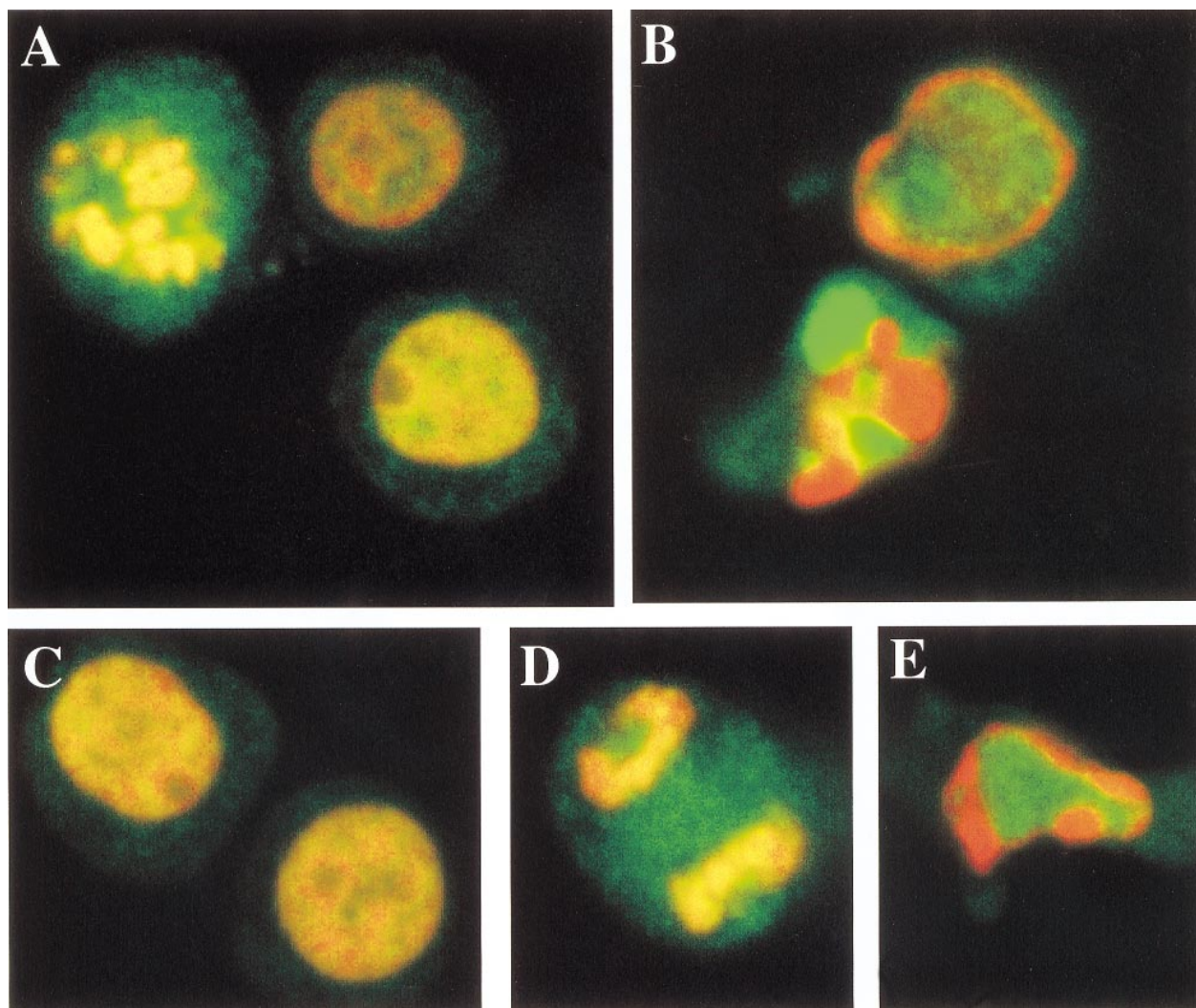


**Fig 7.** Topo II $\alpha$  and II $\beta$  are dissociated from the chromatin during apoptosis. Logarithmically growing (A, C, and D) and apoptotic HL-60 cells treated with Ara-C for 5 hours (B and E) are immunostained with topo II $\alpha$ -specific 8D2 (A and B) and topo II $\beta$ -specific 3G3 monoclonal antibodies (C through E). Topo II $\alpha$  and II $\beta$  signals are green arising from the FITC-conjugated secondary antibody, and PI counterstaining for DNA is red.

especially several hours after the release from serum starvation.<sup>18</sup> Treatment such as serum starvation might also influence the cell viability or topo II levels. Another study, in which cell size was regarded to reflect the cell cycle position, fractionated an asynchronous cell population by centrifugal elutriation and then measured the topo II $\alpha$  level of each fraction.<sup>19</sup> We believe that the two-dimensional flow cytometry determines topo II $\alpha$  and II $\beta$  levels more precisely as functions of the cell cycle position. Our results clearly showed the steep increase of topo II $\alpha$  level in late S to G2/M phases, which correlates well with the known topo II function in chromosome condensation and segregation.<sup>1-4</sup> Some of the G1 cells expressed a larger amount of topo II $\alpha$  than the early S cells. This observation supports the previous hypothesis that topo II $\alpha$  should be degraded from anaphase to early G1 phase until the topo II $\alpha$  level becomes quite low.<sup>19,22</sup> Although both topo II $\alpha$  and II $\beta$  antigens were recently reported to be twofold to threefold higher in mitosis than in interphase, careful examination of the report's data

showed that topo II $\beta$  band intensity increases only from G1 to S phases and thereafter is not significantly altered.<sup>16</sup> This agrees well with our observation that the topo II $\beta$  content is almost constant after G1 phase. We suppose that the topo II $\beta$  content decreases to 50% after cell division and returns to the previous level during G1 phase.

Two-dimensional flow cytometry showed the appearance of a new cell population containing tetraploid DNA and essentially no topo II $\alpha$  during differentiation. Because microscopic examination confirmed that less than 0.3% of the cells were in mitosis at day 6 of the ATRA treatment (data not shown), the new population should be in G2 phase. This cell group was not detected in logarithmically growing cells. These G2 cells are presumed to be noncycling and alive for the following reasons. First, they do not seem to proceed along the cell cycle further, because a sizable amount of topo II $\alpha$  is necessary for the initiation of chromatin condensation in early M phase.<sup>4,5</sup> Second, this population increased in cell number from day 4 to



day 6 of the ATRA treatment, although the cell influx from the S phase must have decreased. This indicates that these cells really stayed at the same stage in the cell cycle. Third, the results from the TUNEL assay on the same differentiated HL-60 samples showed that the apoptotic population was small and restricted to the sub-G1 position (data not shown). We therefore believe that the two-dimensional analysis of our system first clearly detected a G2-arrested nonapoptotic population during the course of differentiation. Because G2 arrest has mainly been studied as a cellular response to DNA damage,<sup>38</sup> little is known about the differentiation-induced G2 arrest. Apigenin, a flavone, was reported to cause both G2 arrest and morphologic differentiation in rat neuronal cells.<sup>39</sup> Another report showed that even irradiation-induced G2 arrest leads to  $\kappa$  light chain gene expression, a sign of differentiation, in 70Z/3 pre-B-cell line.<sup>40</sup> Therefore, G2 arrest seems to induce differentiation in some kinds of cells. Because ATRA does not directly block G2/M transition, our result indicates that cell differentiation itself induces G2 arrest. It seems interesting to determine whether differentiation-induced G2 arrest is a general phenomenon. Cell growth and differentiation are tightly coupled in hematopoietic cells of myeloid lineage, and the half-life of peripheral granulocytes is only a few days.<sup>41</sup> ATRA treatment induces differentiation and subsequent spontaneous cell death even in acute promyelocytic leukemia (APL) cells.<sup>42</sup> Because G2-arrested HL-60 cells are terminally differentiated, they are supposed to undergo apoptosis in a few days.

Two-dimensional flow cytometric analysis of topo II $\beta$  staining (5A7 or 3G3) and TUNEL assay indicated that only the C-terminal portion but not the entire molecule of topo II $\beta$  should be degraded in apoptotic cells. Western blot analysis of Ara-C-treated HL-60 cells using 3G3 clearly showed the proteolytic cleavage of topo II $\beta$  during apoptosis. Comparison of the 5A7 and 3G3 blots confirms that the cleaved topo II $\beta$  fragments retained a central portion but lost the C-terminal 5A7 epitope. On the contrary, a large portion of topo II $\alpha$  remained of its original size even in an advanced stage of apoptosis. The consistency between the results of flow cytometric analysis and Western blotting argues against a possibility that changes in chromatin structure and topo II conformation during apoptosis could affect the topo II $\alpha$  and II $\beta$  stainabilities in the flow cytometric analysis. A previous report showed degradation of topo II enzymes during CD95 (Fas/APO-1) -mediated T-cell apoptosis using a rabbit antibody reactive to both isoforms.<sup>32</sup> A closer look at its data shows that topo II $\beta$  disappears at an early phase of apoptosis and that topo II $\alpha$  remained at its original size even in the advanced stage, although its band became rather faint. The sizes of the topo II degradation products in this report were very similar to those of topo II $\beta$  fragments detected in our study. Another report showed a relatively earlier loss of topo II $\beta$  than topo II $\alpha$  during drug-induced apoptosis in HL-60 and KG1A, although topo II degradates were not detected.<sup>31</sup> Therefore, we believe that degradation of topo II $\beta$  but not of topo II $\alpha$  is a specific and relatively early event in the drug-induced apoptosis.

Both topo II $\alpha$  and II $\beta$  were dissociated from the chromatin at an early phase of apoptosis and completely separated from the genomic DNA in an advanced stage. The degraded topo II $\beta$  fragments, which lost the C-terminal portion, specifically left

the nuclear fraction and dissociated from the chromatin in apoptotic HL-60 cells. This suggests the possible cause-and-effect relationship between the two events. Indeed, some reports indicate that the C-terminal domain itself or its phosphorylation is important for the stability of topo II-DNA interaction.<sup>43,44</sup> Topo II $\alpha$  was also dissociated from the chromatin at an early phase of apoptosis, although a large portion of the enzyme seemed intact, at least by Western blot analysis. This observation suggests that alternative mechanisms might be operating to release topo II $\alpha$  and maybe also topo II $\beta$  from the chromatin. Several nuclear proteins, including nuclear lamin, PARP, and DNA-PKcs, are inactivated by the degradation of their catalytic sites during apoptosis. Topo II $\alpha$  and II $\beta$  are unique in that not the apoptotic proteolysis of their catalytic sites, which reside in the first 1,400 amino acids,<sup>1,2</sup> but their release from the chromatin abolishes the topo II enzyme activity during apoptosis.

Confocal microscopic study confirmed topo II $\alpha$  and II $\beta$  distribution in the nucleus except the nucleoli during interphase of growing HL-60 cells. In mitotic HL-60 cells, both topo II isozymes were distributed throughout the cells and topo II $\alpha$  signal was densely concentrated in the chromosomes, which coincides well with the notion that at least topo II $\alpha$  is not only a necessary enzyme for the chromatin condensation but also a structural component of the mitotic chromosomes.<sup>45-47</sup> Our observation agrees with a recent report on the point that topo II $\beta$  is not preferentially localized in the nucleoli.<sup>16</sup> Although the report further indicated that topo II $\beta$  is completely excluded from the chromosomes during mitosis, we detected topo II $\beta$  signal not only in the mitotic cytoplasm but also in the chromosomes. Monoclonal antibody 5A7 besides 3G3 confirmed that a portion of topo II $\beta$  is localized in the mitotic chromosomes (data not shown). Topo II $\beta$  has furthermore been shown to be present in the isolated chromosomes, albeit in smaller quantities than topo II $\alpha$ .<sup>47</sup> We believe that topo II $\beta$  is at least partially distributed in the mitotic chromosomes. In Ara-C-treated HL-60 cells, topo II $\alpha$  and II $\beta$  were dissociated from the chromatin even at an early phase of apoptosis and were completely excluded from the condensed apoptotic bodies. These observations indicate that dramatic chromatin condensation during apoptosis is entirely topo II-independent. An essential difference must therefore exist between mitotic and apoptotic chromatin condensation.

Differentiation and apoptosis are the two principal cell fates that follow proliferation after cells exit from the cell cycle. Using the HL-60 human leukemia cell line as a model, we have shown the specific loss of topo II $\alpha$  during differentiation and the degradation of topo II $\beta$  even at an early phase of apoptosis. We believe that this study has clarified the different behavior of two topo II isozymes. As previously proposed,<sup>17-21</sup> our results suggest that topo II $\alpha$  plays an essential role in cell proliferation, especially during late S to M phases. In contrast, topo II $\beta$  might be necessary for cell survival because it exists at a substantial level even in the differentiated cells and is degraded early and specifically during apoptosis. Because hematologic malignancies are currently treated by inducing apoptosis or differentiation, monitoring the topo II $\alpha$  and II $\beta$  levels in human leukemia samples may be useful to evaluate the effects of cytotoxic and differentiation therapies.

## ACKNOWLEDGEMENT

The authors thank Drs Tetsuya Nakamoto and Tokiharu Takahashi (the Third Department of Internal Medicine, Faculty of Medicine, University of Tokyo, Tokyo, Japan) and Dr Katsuhiko Kitsugi (Ortho Clinical Diagnostics, Tokyo, Japan) for their technical advice and Dr Masahiro Kizaki (Division of Hematology, Keio University School of Medicine, Tokyo, Japan) for providing us with HL-60 human myeloid leukemia cell line.

## REFERENCES

1. Wang JC: DNA topoisomerases. *Annu Rev Biochem* 65:635, 1996
2. Watt PM, Hickson ID: Structure and function of type II DNA topoisomerases. *Biochem J* 303:681, 1994
3. Uemura T, Ohkura H, Adachi Y, Morino K, Shiozaki K, Yanagida M: DNA topoisomerase II is required for condensation and separation of mitotic chromosomes in *S. pombe*. *Cell* 50:917, 1987
4. Adachi Y, Luke M, Laemmli UK: Chromosome assembly in vitro: Topoisomerase II is required for condensation. *Cell* 64:137, 1991
5. Ishida R, Sato M, Narita T, Utsumi KR, Nishimoto T, Morita T, Nagata H, Andoh T: Inhibition of DNA topoisomerase II by ICRF-193 induces polyploidization by uncoupling chromosome dynamics from other cell cycle events. *J Cell Biol* 126:1341, 1994
6. Liu LF: DNA topoisomerase poisons as antitumor drugs. *Annu Rev Biochem* 58:351, 1989
7. Hunger SP, Tkachuk DC, Amylon MD, Link MP, Carroll AJ, Welborn JL, Willman CL, Cleary ML: *HRX* involvement in de novo and secondary leukemias with diverse chromosome 11q23 abnormalities. *Blood* 81:3197, 1993
8. Gill Super HJ, McCabe NR, Thirman M, Larson RA, Le Beau MM, Pedersen-Bjergaard J, Preben P, Diaz M, Rowley JD: Rearrangements of the *MLL* gene in therapy-related acute myeloid leukemia in patients previously treated with agents targeting DNA-topoisomerase II. *Blood* 82:3705, 1993
9. Broeker PLS, Gill Super H, Thirman MJ, Pomykala H, Yonebayashi Y, Tanabe S, Zeleznik-Le N, Rowley JD: Distribution of 11q23 breakpoints within the *MLL* breakpoint cluster region in de novo acute leukemia and in treatment-related acute myeloid leukemia: Correlation with scaffold attachment regions and topoisomerase II consensus binding sites. *Blood* 87:1912, 1996
10. Aplan PD, Chervinsky DS, Stanulla M, Burhans WC: Site-specific DNA cleavage within the *MLL* breakpoint cluster region induced by topoisomerase II inhibitors. *Blood* 87:2649, 1996
11. Jenkins JR, Ayton P, Jones T, Davies SL, Simmons DL, Harris AL, Sheer D, Hickson ID: Isolation of cDNA clones encoding the  $\beta$  isozyme of human DNA topoisomerase II and localization of the gene to chromosome 3p24. *Nucleic Acids Res* 20:5587, 1992
12. Austin CA, Sng J-H, Patel S, Fisher M: Novel HeLa topoisomerase II is the II $\beta$  isoform: Complete coding sequence and homology with other type II topoisomerases. *Biochim Biophys Acta* 1172:283, 1993
13. Negri C, Chiesa R, Cerino A, Bestagno M, Sala C, Zini N, Maraldi NM, Astaldi Ricotti GCB: Monoclonal antibodies to human DNA topoisomerase I and the two isoforms of DNA topoisomerase II: 170- and 180-kDa isozymes. *Exp Cell Res* 200:452, 1992
14. Petrov P, Drake FH, Loranger A, Huang W, Hancock R: Localization of DNA topoisomerase II in Chinese hamster fibroblasts by confocal and electron microscopy. *Exp Cell Res* 204:73, 1993
15. Zini N, Martelli AM, Sabatelli P, Santi S, Negri C, Astaldi Ricotti GCB, Maraldi NM: The 180-kDa isoform of topoisomerase II is localized in the nucleolus and belongs to the structural elements of the nucleolar remnant. *Exp Cell Res* 200:460, 1992
16. Meyer KN, Kjeldsen E, Straub T, Knudsen BR, Hickson ID, Kikuchi A, Kreipe H, Boege F: Cell cycle-coupled relocation of types I and II topoisomerases and modulation of catalytic enzyme activities. *J Cell Biol* 136:775, 1997
17. Drake FH, Hofmann GA, Bartus HF, Mattern MR, Crooke ST, Mirabelli CK: Biochemical and pharmacological properties of p170 and p180 forms of topoisomerase II. *Biochemistry* 28:8154, 1989
18. Woessner RD, Mattern MR, Mirabelli CK, Johnson RK, Drake FH: Proliferation- and cell cycle-dependent differences in expression of the 170 kilodalton and 180 kilodalton forms of topoisomerase II in NIH-3T3 cells. *Cell Growth Differ* 2:209, 1991
19. Heck MMS, Hittelman WN, Earnshaw WC: Differential expression of DNA topoisomerases I and II during the eukaryotic cell cycle. *Proc Natl Acad Sci USA* 85:1086, 1988
20. Heck MMS, Earnshaw WC: Topoisomerase II: A specific marker for cell proliferation. *J Cell Biol* 103:2569, 1986
21. Kaufmann SH, McLaughlin SJ, Kastan MB, Liu LF, Karp JE, Burke PJ: Topoisomerase II levels during granulocytic maturation in vitro and in vivo. *Cancer Res* 51:3534, 1991
22. Nakajima T, Ohi N, Arai T, Nozaki N, Kikuchi A, Oda K: Adenovirus E1A-induced apoptosis elicits a steep decrease in the topoisomerase II $\alpha$  level during the latent phase. *Oncogene* 10:651, 1995
23. Kerr JFR, Wyllie AH, Currie AR: Apoptosis: A basic biological phenomenon with wide-ranging implications in tissue kinetics. *Br J Cancer* 26:239, 1972
24. Wyllie AH, Kerr JFR, Currie AR: Cell death: The significance of apoptosis. *Int Rev Cytol* 68:251, 1980
25. Lazebnik YA, Cole S, Cooke CA, Nelson WG, Earnshaw WC: Nuclear events of apoptosis in vitro in cell-free mitotic extracts: A model system for analysis of the active phase of apoptosis. *J Cell Biol* 123:7, 1993
26. Kumar S: ICE-like proteases in apoptosis. *Trends Biochem Sci* 20:198, 1995
27. Martin SJ, Green DR: Protease activation during apoptosis: Death by a thousand cuts. *Cell* 82:349, 1995
28. Lazebnik YA, Kaufmann SH, Desmoyens S, Poirier GG, Earnshaw WC: Cleavage of poly (ADP-ribose) polymerase by a proteinase with properties like ICE. *Nature* 371:346, 1994
29. Lazebnik YA, Takahashi A, Moir RD, Goldman RD, Poirier GG, Kaufmann SH, Earnshaw WC: Studies of the lamin proteinase reveal multiple parallel biochemical pathways during apoptotic execution. *Proc Natl Acad Sci USA* 92:9042, 1995
30. Song Q, Lees-Miller SP, Kumar S, Zhang N, Chan DW, Smith GCM, Jackson SP, Alnemri ES, Litwack G, Khanna KK, Lavin MF: DNA-dependent protein kinase catalytic subunit: A target for an ICE-like protease in apoptosis. *EMBO J* 15:3238, 1996
31. Kaufmann SH: Induction of endonucleolytic DNA cleavage in human acute myelogenous leukemia cells by etoposide, camptothecin, and other cytotoxic anticancer drugs: A cautionary note. *Cancer Res* 49:5870, 1989
32. Casiano CA, Martin SJ, Green DR, Tan EM: Selective cleavage of nuclear autoantigens during CD95 (Fas/APO-1)-mediated T cell apoptosis. *J Exp Med* 184:765, 1996
33. Kimura K, Nozaki N, Saijo M, Kikuchi A, Ui M, Enomoto T: Identification of the nature of modification that causes the shift of DNA topoisomerase II $\beta$  to apparent higher molecular weight forms in the M phase. *J Biol Chem* 269:24523, 1994
34. Gorczyca W, Gong J, Darzynkiewicz Z: Detection of DNA strand breaks in individual apoptotic cells by the in situ terminal deoxynucleotidyl transferase and nick translation assays. *Cancer Res* 53:1945, 1993
35. Towbin H, Staehelin T, Gordon J: Electrophoretic transfer of proteins from polyacrylamide gels to nitrocellulose sheets: procedure and some applications. *Proc Natl Acad Sci USA* 76:4350, 1979
36. Chabner BA, Allegra CJ, Curt GA, Calabresi P: Antineoplastic agents, in Hardman JG, Limbird LE, Molinoff PB, Ruddon RW, Gilman AG: Goodman and Gilman's The Pharmacological Basis of Therapeutics (ed 9). New York, NY, McGraw-Hill, 1996, p 1233

37. Gorczyca W, Gong J, Ardel B, Traganos F, Darzynkiewicz Z: The cell cycle related differences in susceptibility of HL-60 cells to apoptosis induced by various antitumor agents. *Cancer Res* 53:3186, 1993
38. Jin P, Gu Y, Morgan DO: Role of inhibitory CDC2 phosphorylation in radiation-induced G2 arrest in human cells. *J Cell Biol* 134:963, 1996
39. Sato F, Matsukawa Y, Matsumoto K, Nishino H, Sakai T: Apigenin induces morphological differentiation and G2-M arrest in rat neuronal cells. *Biochem Biophys Res Commun* 204:578, 1994
40. Aloni-Grinstein R, Schwartz D, Rotter V: Accumulation of wild-type p53 protein upon  $\gamma$ -irradiation induces a G2 arrest-dependent immunoglobulin  $\kappa$  light chain gene expression. *EMBO J* 14:1392, 1995
41. Abboud CN, Liesveld JL: Granulopoiesis and monocytopoiesis, in Hoffman R, Benz EJ, Shattil SJ, Furie B, Cohen HJ, Silberstein LE (eds): *Hematology: Basic Principles and Practice* (ed 2). New York, NY, Churchill Livingstone, 1995, p 255
42. Warrell RP, De Thé H, Wang Z-Y, Degos L: Acute promyelocytic leukemia. *N Engl J Med* 329:177, 1993
43. Crenshaw DG, Hsieh T: Function of the hydrophilic carboxyl terminus of type II topoisomerase from *Drosophila melanogaster*. I: In vitro studies. *J Biol Chem* 268:21328, 1993
44. Dang Q, Alghisi GC, Gasser SM: Phosphorylation of the C-terminal domain of yeast topoisomerase II by casein kinase II affects DNA-protein interaction. *J Mol Biol* 243:10, 1994
45. Earnshaw WC, Halligan B, Cooke CA, Heck MMS, Liu LF: Topoisomerase II is a structural component of mitotic chromosome scaffolds. *J Cell Biol* 100:1706, 1985
46. Gasser SM, Laroche T, Falquet J, Boy de la Tour E, Laemmli UK: Metaphase chromosome structure: Involvement of topoisomerase II. *J Mol Biol* 188:613, 1986
47. Taagepera S, Rao PN, Drake FH, Gorbsky GJ: DNA topoisomerase II $\alpha$  is the major chromosome protein recognized by the mitotic phosphoprotein antibody MPM-2. *Proc Natl Acad Sci USA* 90:8407, 1993